ELSEVIER

Thermochimica Acta 340–341 (1999) 367–376

thermochimica acta

www.elsevier.com/locate/tca

The relationship between stoichiometry and reactivity for violarite

A.C. Chamberlain[a,*], J.G. Dunn[b,1]

[a]*WMC Resources Limited, Mineral Processing Group, Nickel Division, Perth, Australia*
[b]*School of Applied Chemistry, Curtin University of Technology, Perth, Australia*

Accepted 6 August 1999

Abstract

Four samples of violarite, of compositions $Fe_{0.20}Ni_{2.72}S_4$, $Fe_{0.46}Ni_{2.49}S_4$, $Fe_{0.73}Ni_{2.26}S_4$ and $Fe_{0.97}Ni_{1.96}S_4$, were synthesised and characterised. Each sample was fractionated into four, with particle sizes of 125–90, 90–63, 63–45 and <45 μm. The samples were ignited in a TG apparatus, and the effects of change in stoichiometry and particle size on the ignition temperature, and extent of oxidation at a specific temperature, determined. Samples of the ignited material were taken at various temperatures, and their properties examined using scanning electron microscopy, optical microscopy and electron probe microanalysis. The results enabled an ignition mechanism for violarite to be proposed.

Keywords: Extent of oxidation; Ignition temperature; Mechanism of ignition; Particle size; Stoichiometry; Violarite

1. Introduction

Violarite, of general formula $(Ni,Fe)_3S_4$, is an economically important source of nickel. It normally occurs as a secondary mineral resulting from supergene alteration of other nickel sulfides. Three distinct mechanisms have been identified for its formation.

The first mechanism involves alteration of both pentlandite, $(Fe,Ni)_9S_8$, and pyrrhotite, (FeS), with the formation of violarite and pyrite (FeS_2) [1,2], and can be represented by the following general equations [1]:

$$Fe_{4.1}Ni_{4.9}S_8 \rightarrow 2Fe_{1.3}Ni_{1.9}S_4 + 1.1Ni^{2+} + 1.5Fe^{2+} + 5.2e^-$$
$$0.33Fe_7S_8 + 1.1Ni^{2+} \rightarrow 0.66Fe_{1.5}Ni_{1.7}S_4 + 1.3Fe^{2+} + 0.4e^-$$
$$Fe_7S_8 \rightarrow 4FeS_2 + 3Fe^{2+} + 6e^-$$

The driving force for the above anodic reactions is the cathodic reduction of oxygen and water at the water table.

The second mechanism involves alteration of millerite–pentlandite (NiS–$(Fe,Ni)_9S_8$) assemblages. The oxidation of millerite is limited by the quantity of iron available from the oxidation of pentlandite.

$$Fe_{3.6}Ni_{5.4}S_8 \rightarrow 2Fe_{0.5}Ni_{2.7}S_4 + 2.6Fe^{2+} + 5.2e^-$$
$$20.8NiS + 2.6Fe^{2+} \rightarrow 5.2Fe_{0.5}Ni_{2.7}S_4 + 6.8Fe^{2+} + 8.4e^-$$

Both violarites formed tend to be more nickel-rich than those formed from pyrrhotite–pentlandite assemblages.

A third type of mechanism occurs in the later stages of millerite replacement, and gives a product which exhibits an extremely high nickel content with a composition approaching that of polydymite, Ni_3S_4. The relative abundance is only very small [1,3].

*Corresponding author.
[1]Present address: Department of Chemistry, University of Toledo, OH, USA.

0040-6031/99/$ – see front matter
PII: S0040-6031(99)00282-8

Consequently, as a result of these various reactions, natural violarites tend to exhibit a wide range of stoichiometries.

One of the processing routes for nickel bearing sulfides is to ignite the sulfide particles in a flash smelter. It has already been demonstrated that the ignition temperature of pyrrhotite varies significantly with stoichiometry [4]. The present work was undertaken to study the effect of changing stoichiometry on the reactivity of violarite. Unfortunately, it is not easy to separate high purity violarite samples from naturally occurring minerals, and so a series of synthetic violarites were prepared. Their ignition temperatures were determined using a previously described isothermal TG technique [5].

2. Experimental

2.1. Synthesis of iron–nickel sulfides

A two-stage synthesis was employed to form homogeneous violarite with a general composition of $(Fe,Ni)_3S_4$. The first stage involved the production of a monosulphide solid solution (MSS) of the required composition, followed by a second stage in which the violarite phase was formed. The procedure was based on previously described methods [6,7]. Iron, nickel and sulfur of greater than 99.99% purity were obtained from Aldrich chemical. All experiments were performed using Vycor® glass tubing obtained from Corning.

2.2. Characterisation of violarite samples

The percentage iron, nickel and sulfur in each sample were determined using classical wet chemical techniques. The results are presented in Table 1, together with the calculated stoichiometries of the four samples.

The structure and composition of each sample was confirmed by X-ray diffraction (XRD) and electron probe microanalysis (EPMA).

Each sample was dry sieved through a stack of Brass Endecott Laboratory Test Sieves to isolate four fractions, 125–90, 90–63, 63–45 and <45 μm.

2.3. Ignition temperature measurements

Ignition temperature measurements were performed using a Stanton–Redcroft TG-750 thermobalance. Approximately 5 mg of sample was weighed into a platinum sample crucible, measuring 5 mm in diameter and 2 mm in depth. An oxygen atmosphere at a flowrate of 25 ml min^{-1} was established. The furnace was preheated to a set temperature between 400°C and 900°C, and raised on a cam shaft around the sample. The ignition temperature of each sample was measured by increasing the temperature of the furnace at 5°C increments until the sample underwent ignition and a rapid mass loss was observed.

The extent of reaction was also determined. The maximum weight loss was found to occur when the sample was inserted into the furnace preheated to 900°C, and corresponded to complete oxidation of the sample. By measuring the mass loss at any furnace temperature below 900°C, the following formula could be used to calculate the percent extent of reaction at that temperature.

$$\text{Percent extent of reaction} = \frac{100(\text{weight loss at any temperature, } T^{\circ}\text{C})}{(\text{weight loss at } 900^{\circ}\text{C})}.$$

Table 1
Results of wet chemical analysis for synthetic violarites

Sample	Composition (wt.%)				Stoichiometry
	Fe	Ni	S	Total	
1	18.24	38.66	43.34	100.24	$Fe_{0.97 \pm 0.01}Ni_{1.96 \pm 0.02}S_{4 \pm 0.03}$
2	13.54	43.98	44.19	101.71	$Fe_{0.73 \pm 0.01}Ni_{2.26 \pm 0.02}S_{4 \pm 0.03}$
3	8.59	48.69	43.98	101.26	$Fe_{0.46 \pm 0.01}Ni_{2.49 \pm 0.02}S_{4 \pm 0.03}$
4	3.74	53.32	43.39	100.45	$Fe_{0.20 \pm 0.01}Ni_{2.72 \pm 0.02}S_{4 \pm 0.03}$

3. Results and discussion

3.1. Effect of stoichiometry on ignition temperature

The ignition temperatures of the four violarite samples of four differing particle sizes were determined using the isothermal TG method, and the results are presented in Fig. 1.

There is a clear relationship between the iron:nickel ratio of synthetic violarite and the ignition temperature. For example, there was an increase in the ignition temperature from 415°C to 435°C for the end members of the violarite solid solution, $Fe_{0.97}Ni_{1.96}S_4$ and $Fe_{0.20}Ni_{2.72}S_4$, for the 63–45 μm particle size fraction. However, the effect of stoichiometry on the ignition temperature was not linearly dependent. The violarite samples became increasingly more difficult to ignite as the stoichiometry approached the nickel-rich end-member of the violarite solid solution.

The relative order of reactivity of the synthetic violarite series was established as:

$$Fe_{0.97}Ni_{1.96}S_4 > Fe_{0.73}Ni_{2.26}S_4 > \underset{\leftarrow}{Fe_{0.46}Ni_{2.49}S_4} > Fe_{0.20}Ni_{2.72}S_4$$

Increase in reactivity as iron:nickel ratio increase.

The values obtained were in general close agreement to those measured for natural violarite samples of 400°C [8], and 430°C [9], although these samples were not of the same purity as the synthetic ones. In

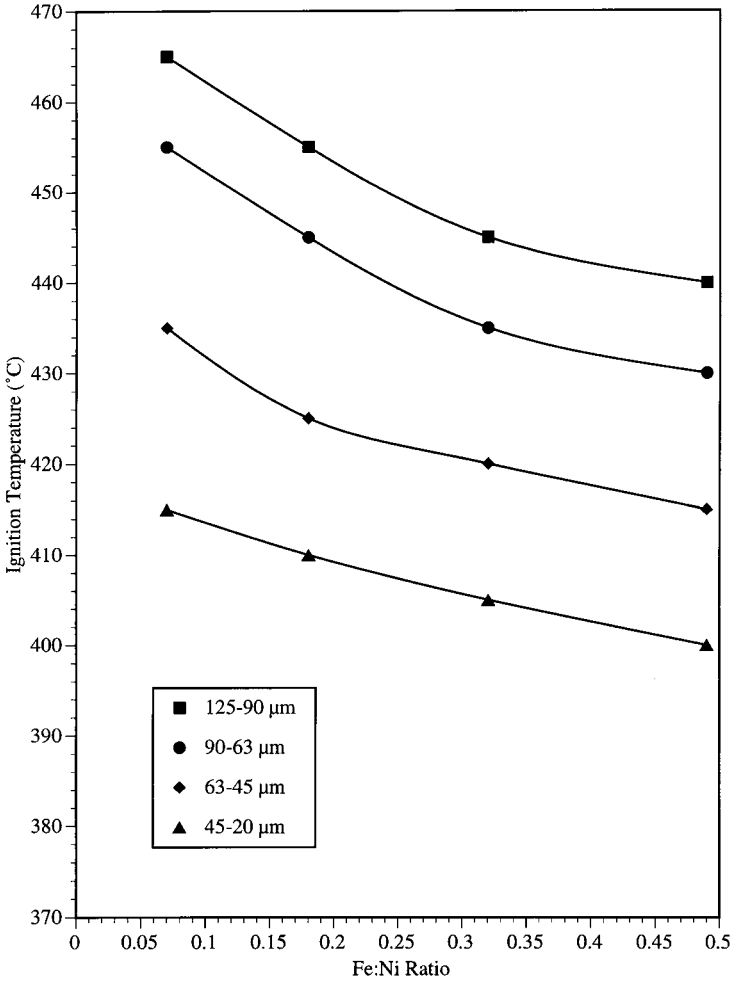

Fig. 1. Effect of Fe:Ni ratio on the ignition temperature of the four violarite samples for a range of particle sizes.

addition, natural minerals, especially those formed by supergene alteration, tend to have higher surface areas than those synthesised in the current study. Therefore, ignition temperatures for natural samples may be lower than those of their synthetic equivalents.

3.2. Effect of particle size on the ignition temperature of violarite

The effect of particle size on the ignition temperature was investigated using all four violarite samples, and the results shown in Fig. 1 have been replotted in Fig. 2 to emphasise the effect.

The violarite samples showed a decrease in ignition temperature as the particle size decreased. For example, the ignition temperature of $Fe_{0.97}Ni_{1.96}S_4$ decreased from 440°C to 400°C between the coarsest and finest particle size fractions.

The iron:nickel ratio also influenced the effect of particle size on the ignition temperature (Fig. 2). For example, the ignition temperature of $Fe_{0.20}Ni_{2.72}S_4$ decreased by 50°C compared with 40°C for

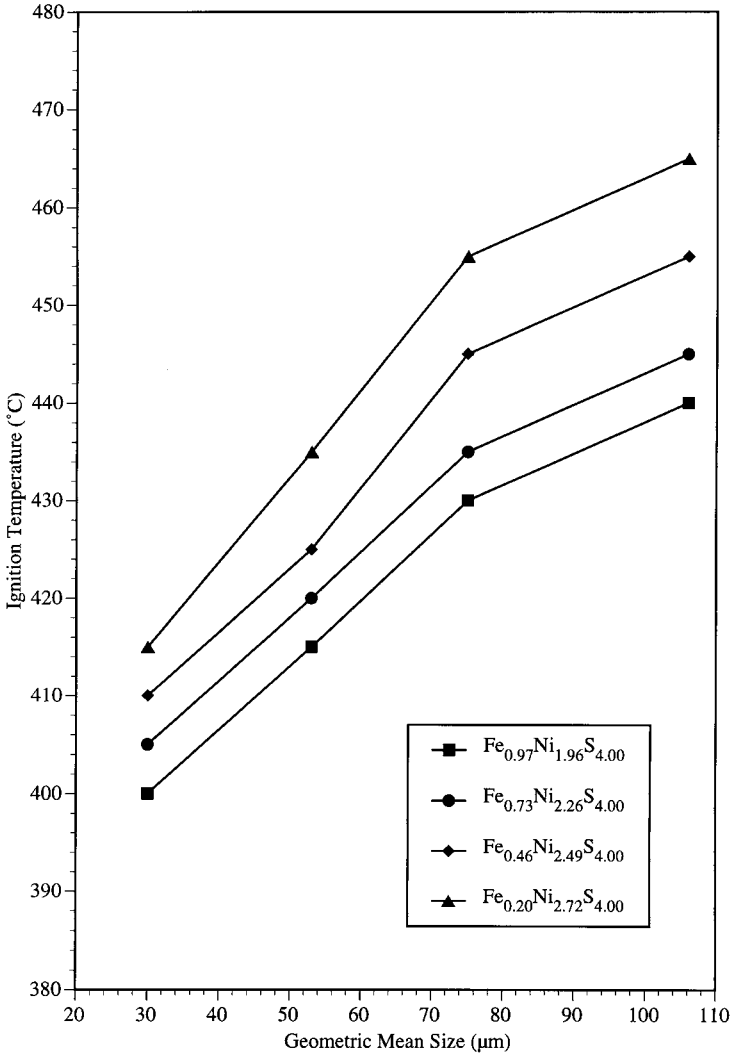

Fig. 2. Effect of particle size on the ignition temperature for the four violarite samples.

$Fe_{0.97}Ni_{1.96}S_4$. Therefore, the effect of particle size increased as the stoichiometry of the violarite tended towards the nickel-rich end of the violarite solid solution. This is evident also from Fig. 2, which shows that the ignition temperature curves converge as the particle size decreases.

Hence, the effect of particle size on ignition behaviour of synthetic violarite decreased in the following order:

$$Fe_{0.20}Ni_{2.72}S_4 > Fe_{0.46}Ni_{2.49}S_4 > Fe_{0.73}Ni_{2.26}S_4 = Fe_{0.97}Ni_{1.96}S_4.$$

The difference in the ignition temperatures between $Fe_{0.97}Ni_{1.96}S_4$ and $Fe_{0.20}Ni_{2.72}S_4$ is 25°C for the 125–90 μm particle size fraction and 15°C for the 45–20 μm fraction. Hence, the effect of stoichiometry can be minimised by a reduction in particle size.

3.3. Determination of the extent of oxidation by isothermal TG

The extent of oxidation of synthetic violarite was determined by the isothermal TG technique [5], as outlined in Section 2.3. Fig. 3 shows the effect of

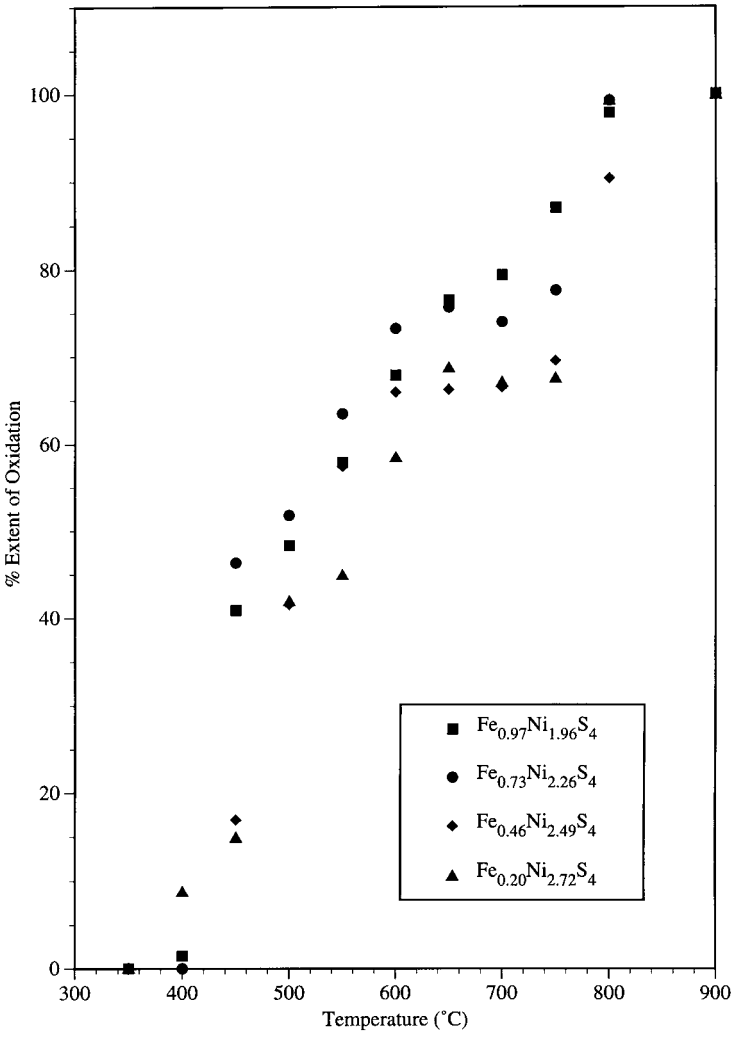

Fig. 3. The effect of stoichiometry on the extent of oxidation for the 63–45 μm particle size fraction of the four violarite samples.

stoichiometry on the extent of oxidation for the four violarite samples for particle size range of 63–45 μm. The extent of oxidation prior to the ignition temperature was minimal, but a rapid increase was observed once the ignition temperatures were achieved. $Fe_{0.97}Ni_{1.96}S_4$ underwent a 7.95% mass loss at its ignition temperature. A total mass loss of 24.8% was observed at 900°C, which agrees with the theoretical mass loss of 24.8% that would be observed if violarite were fully oxidised to hematite (Fe_2O_3) and nickel oxide (NiO). Therefore, the percent extent of reaction of $Fe_{0.97}Ni_{1.96}S_4$ at its ignition temperature was 32%.

The two iron-rich violarite samples, $Fe_{0.97}Ni_{1.96}S_4$ and $Fe_{0.73}Ni_{2.26}S_4$, had undergone a greater extent of oxidation than the nickel-rich samples between the temperature range 400–650°C. For example, at 500°C $Fe_{0.97}Ni_{1.96}S_4$ had oxidised 48% while $Fe_{0.20}Ni_{2.72}S_4$ had only oxidised 42%. The extent and rate of oxidation decreased as the iron nickel ratio decreased between 650°C and 750°C. For example, $Fe_{0.97}Ni_{1.96}S_4$ showed an increase in the extent of oxidation from 76% to 87% over the temperature range 650–750°C, while the extent of oxidation for $Fe_{0.20}Ni_{2.72}S_4$ remained relatively constant at 68% over the same temperature range. As the temperature of the furnace was increased above 750°C, the extent of oxidation increased with all four samples approaching 100% oxidation by 800°C.

Hence, the stoichiometry of the violarite has an effect on the extent of oxidation in the middle temperature range of 400–750°C, with the extent of oxidation increasing with an increase in the iron:-nickel ratio of the sulfide. The effect of stoichiometry became less significant as the temperature was increased above 750°C.

Tables 2 and 3 give the extent of reaction for $Fe_{0.97}Ni_{1.96}S_4$ and $Fe_{0.20}Ni_{2.72}S_4$ for the four particle sizes. The results indicate a greater particle size effect in the lower temperature range. $Fe_{0.97}Ni_{1.96}S_4$ had only undergone 8% oxidation at 450°C for the 125–90 μm particle size fraction compared with 40% for the 45–20 μm fraction. By 500°C, the extent of oxidation for the two respective particle size fractions was 53% and 52%. For $Fe_{0.20}Ni_{2.72}S_4$ at 500°C, the 125–90 μm fraction had oxidised by 14% compared with 41% oxidation for the 45–20 μm particle size fraction. By 600°C the extent of oxidation had increased significantly, with the coarser particle size fraction showing an increased extent of reaction from 14% to 64%, an increase of 50%. This can be compared with a 19% increase in the extent of oxidation, from 41% to 60% for the 45–20 μm fraction. Hence, a 100°C increase in the furnace temperature significantly decreased the effect of particle size on the extent of oxidation. The extent of oxidation remained relatively constant between each particle size fraction as the temperature was increased up to 900°C.

Table 2
Extent of oxidation of $Fe_{0.97}Ni_{1.96}S_4$ for each particle size fraction

Temperature (°C)	Particle size fraction (μm)			
	125–90	90–63	63–45	45–20
350	0	0	0	0
400	0	0	1.4	0
450	7.6	5.8	29.7	39.8
500	53.0	43.6	48.3	52.4
550	68.4	57.0	57.9	64.5
600	75.1	71.0	67.8	74.2
650	81.9	77.5	76.5	78.0
700	78.2	82.7	79.4	78.2
750	86.6	87.7	87.0	80.1
800	100.0	98.7	97.8	98.0
900	100.0	100.0	100.0	100.0

Tables 2 and 3 further demonstrate the effect of stoichiometry on the extent of oxidation. The 125–90 μm particle size fraction for $Fe_{0.97}Ni_{1.96}S_4$ had oxidised 82% by 650°C, while $Fe_{0.20}Ni_{2.72}S_4$ had undergone only 66% oxidation at the same temperature. As the temperature increased above 740°C, the

Table 3
Extent of oxidation of $Fe_{0.20}Ni_{2.72}S_4$ for each particle size fraction

Temperature (°C)	Particle size fraction (μm)			
	125–90	90–63	63–45	45–20
350	0	0	0.1	0
400	10.3	10.8	8.8	5.8
450	13.0	18.7	15.0	21.3
500	13.9	36.3	42.0	40.9
550	31.5	37.1	45.0	48.2
600	64.0	50.9	58.6	59.6
650	65.7	63.7	68.8	65.7
700	62.9	64.5	67.1	63.3
750	68.2	65.6	67.6	66.3
800	97.8	97.6	99.4	96.0
900	100.0	100.0	100.0	100.0

effect of stoichiometry decreased as the extent of oxidation approached 100%.

Therefore, the effect of particle size on the extent of oxidation is significant in the lower temperature range of 350–450°C, while the effect of stoichiometry tends to be more important in the mid temperature range of 400–750°C. Above 750°C, particle size and stoichiometry have a limited effect on the extent of oxidation.

3.4. Ignition mechanism of violarite

In order to establish the ignition mechanism, partially oxidised and ignited products from isothermal TG experiments were examined. Due to the furnace design, the samples could be quenched from the ignition temperature to room temperature in a matter of seconds. Samples were collected at 5–10°C prior to the ignition temperature and then at 50°C intervals beyond the ignition temperature up to 900°C. Both polished sections and individual grains were mounted for optical and SEM examination. Mineralogical examination of the ignition products was performed using XRD and EPMA. The studies were carried out on the 63–45 μm size fraction of $Fe_{0.97}Ni_{1.96}S_4$.

The TG profiles for $Fe_{0.97}Ni_{1.96}S_4$ (63–45 μm fraction) at the ignition temperature, 425°C, and at 900°C, are reproduced in Fig. 4. As the furnace temperature was increased above the ignition temperature the TG profile remained unchanged, with the rapid mass loss increasing slightly. Between 650–750°C the extent of oxidation remained constant with no increase in the mass loss. Above 750°C the mass loss occurred in two discrete stages (Fig. 4, right). These results indicate that the reaction proceeded in two steps, with the first stage being typical of an ignition reaction, and the second one being more reminiscent of a reaction controlled by oxygen diffusion. Previous work had established that the first stage was due to the preferential oxidation of iron sulfide, followed by the gradual oxidation of nickel sulfide phases during the second stage [10]. The preferential oxidation of iron in binary sulfides has also been reported for another iron–nickel sulfide [11] as well as an iron–copper sulfide [12].

Examination of $Fe_{0.97}Ni_{1.96}S_4$ just prior to the ignition temperature showed only a minor amount of oxidation. Approximately 10 particles collected

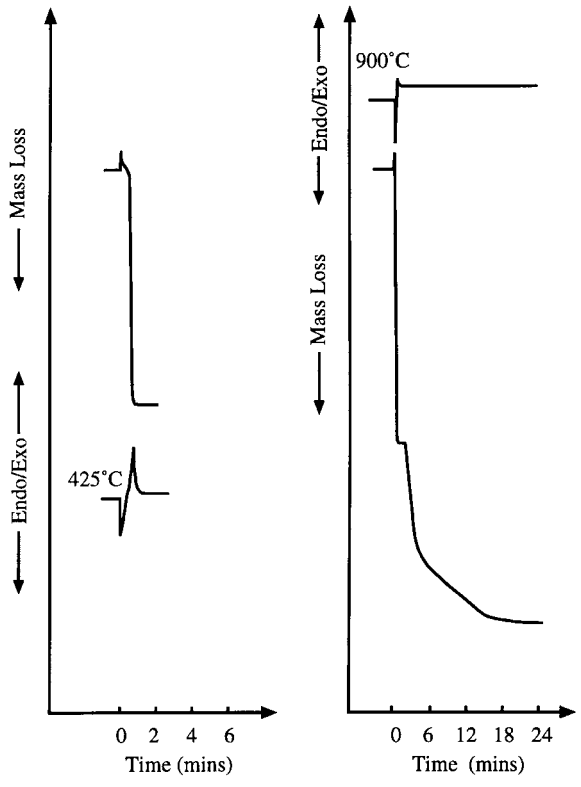

Fig. 4. Typical isothermal TG trace for $Fe_{0.97}Ni_{1.96}S_4$ (63–45 μm fraction) at 425°C and 900°C. Note the different time scales for each plot.

at 420°C were analysed by EPMA. The results indicated that a minor amount of the sample had reverted to a MSS phase, with an average composition of $Fe_{0.35}Ni_{0.58}S_{1.00}$. The violarite composition had changed to $Fe_{1.17}Ni_{1.97}S_{4.00}$. SEM micrographs showed small cracks on the surface of the particles.

At the ignition temperature, the morphology of the sample underwent a dramatic change. Fig. 5a (left) shows a back scattered electron (BSE) micrograph collected at 425°C. The majority of the particles exhibited a porous structure with hematite evident within the particle pores. The degree of porosity varied from particle to particle with the pores penetrating non-uniformly through the MSS core. XRD revealed MSS and hematite as the major phases present, with a minor amount of NiO also present. No violarite was evident in the XRD pattern. There was a large variation in the composition of the MSS phase. Analysis by

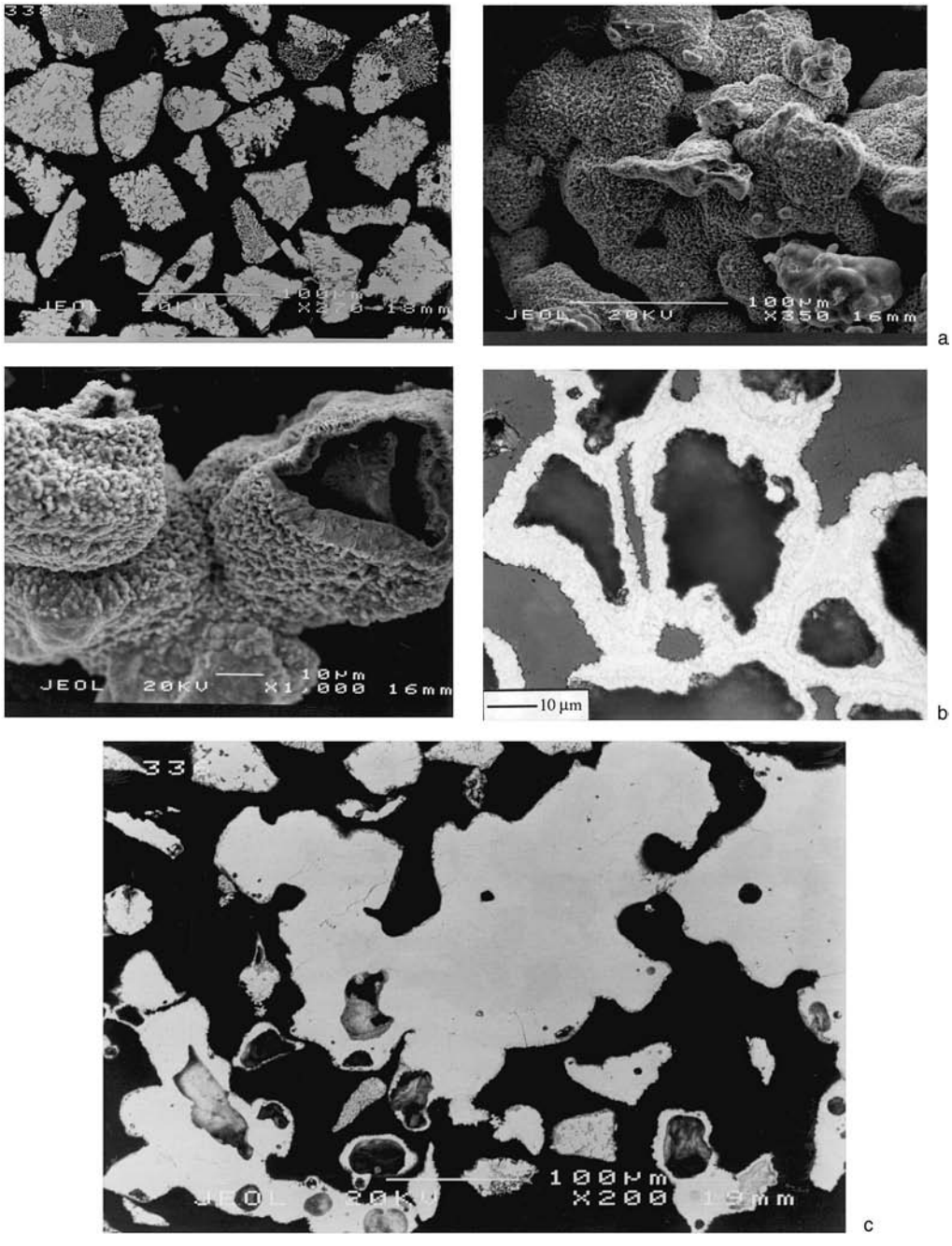

Fig. 5. (a) BSE (left) and SE (right) micrographs of $Fe_{0.97}Ni_{1.96}S_4$, 63–45 μm particle size fraction, at the ignition temperature (425°C). (b) SE (left) and optical (right) micrographs showing molten spheres of heazlewoodite (sample collected at 450°C). (c) BSE micrograph of sample collected at 750°C.

EPMA of approximately 10 particles of $Fe_{0.97}Ni_{1.96}S_4$ showed the MSS stoichiometry ranged from $Fe_{0.32}Ni_{0.67}S_{1.00}$ to $Fe_{0.16}Ni_{0.83}S_{1.00}$ with the iron nickel ratio decreasing between the sulfide core and outer edge of the violarite particle. These results indicated the preferential oxidation of iron sulfides relative to nickel sulfides, and also evidence of the migration of iron towards the surface of the particles [13].

Fig. 5a (right) shows a secondary electron (SE) micrograph of a number of unsectioned particles collected at the ignition temperature. The surfaces of the particles show a random network of pores. The particles formed hollow spheres which resembled cenospheres. A number of particles had fused together forming a molten sulfide mass (Fig. 5b, left). This was probably caused by the ignition reaction raising the temperature of the sample above the furnace temperature. Heazlewoodite, $(Ni,Fe)_3S_2$, one of the previously identified intermediate nickel sulfide phases, has a melting temperature in the range 750–800°C, depending on the iron content [14]. The optical micrograph of the polished section showed the presence of two distinctive phases (Fig. 5b, right). EPMA revealed the bright phase to be heazlewoodite with average composition of $(Fe_{0.31}Ni_{2.79})S_2$. The second darker phase was probably an oxide phase. No accurate analysis of this phase was possible due to the fine grain size, but EPMA results suggested that it was trevorite ($NiFe_2O_4$).

The porosity of the violarite ignition product resembled that of violarite which had decomposed via loss of sulfur vapour when heated in nitrogen [14]. Therefore, the particle morphology suggested that even in the presence of oxygen some of the sample had undergone a similar pyrolytic decomposition prior to any oxidation reaction. A number of other studies have shown that similar morphologies were observed when sulfides were heated in nitrogen or ignited in oxygen [9,15–18]. Hematite was clearly visible within the macropores.

Particles collected above the ignition temperature showed a slight increase in the porosity. As the temperature approached the melting point of heazlewoodite (750–800°C) large molten masses of heazlewoodite were found (Fig. 5c). Some cenosphere formation was also evident in a number of particles. Once the temperature exceeded the melting point transition of heazlewoodite the remaining nickel sulfide was oxidised to completion.

The following reaction mechanism is proposed for the ignition of violarite:

1. *Pyrolytic decomposition of violarite.* It has previously been shown that the 63–45 μm size fraction of $Fe_{0.97}Ni_{1.96}S_4$ decomposes in nitrogen in a three-stage process in the temperature range 420–525°C. In the first stage, there is a loss of sulfur to give a metal rich violarite of typical composition $Fe_{1.14}Ni_{1.86}S_{3.86}$ and MSS. In the second stage the remaining violarite decomposes completely with the formation of vaesite $(Fe,Ni)S_2$ and MSS, resulting in the evolution of more sulfur. Finally, vaesite decomposes to MSS between 600°C and 680°C [14]. It is proposed that the ignition reaction is initiated by the first decomposition step. The evolved sulfur burns at the surface of the particle, which increases the particle temperature as well as inhibiting diffusion of oxygen into the violarite pores. The particle temperature exceeds the decomposition temperature of the second and third reactions, which liberates more sulfur, and the cycle is repeated. The presence of some melted heazlewoodite indicates that some of the sample had been heated to at least 750°C even though the furnace temperature was only set at 425°C.
2. *Preferential oxidation of iron sulfide.* During the ignition reaction, iron migrates towards the outer rim where it is preferentially oxidised leaving a nickel-rich MSS core. The preferential oxidation appears to occur once the partial pressure of the evolved sulfur gas decreases sufficiently to allow the diffusion of oxygen through the porous structure.
3. *Oxidation of remaining sulfide core.* The extent of oxidation of the remaining nickel sulfide increases as the temperature increases. The reaction is limited by the gaseous diffusion of oxygen through the surrounding oxide layer. The reaction goes to completion when the particle temperature exceeds the melting point transition of heazlewoodite. This accounts for the temperature and time dependence of the extent of oxidation of violarite once the iron has been preferentially oxidised.

4. Conclusions

The primary purpose of this work was to study the effect of stoichiometry on the ignition properties of violarite. There was a decrease in reactivity of the violarite samples as the iron:nickel ratio decreased, as indicated by an increase in the ignition temperature and a decrease in the extent of oxidation at a specific temperature. On the other hand, a decrease in particle size decreased the ignition temperature and increased the extent of oxidation. The magnitude of the effect varied with the iron:nickel ratio. The ignition temperature for $Fe_{0.20}Ni_{2.72}S_4$ showed the largest decrease of 50°C between the coarsest and finest particle size fractions, compared with a 40°C decrease for $Fe_{0.97}Ni_{1.96}S_4$.

From an industrial viewpoint, $Fe_{0.97}Ni_{1.96}S_4$ with a particle size of 45–20 μm would be the easiest of the violarite samples to flash smelt, as it had the lowest ignition temperature of 400°C. The most difficult to flash smelt would be $Fe_{0.20}Ni_{2.72}S_4$ with a particle size of 125–90 μm, which ignited at 465°C. Hence, violarites with a small particle size and high iron composition are more readily smelted than those with larger particle sizes and higher nickel contents.

Acknowledgements

ACC expresses his appreciation for an Australian Post Graduate Award (Industry) to carry out the work, and we both thank staff of WMC Resources, Kalgoorlie Nickel Smelter for financial assistance, and much useful discussion and advice.

References

[1] R.A. Keele, E.H. Nickel, Econ. Geology 69 (1974) 1102–1117.
[2] E.H. Nickel, J.R. Ross, M.R. Thornber, Econ. Geology 69 (1974) 93–107.
[3] M.R. Thornber, Chem. Geology 15 (1975) 1–14.
[4] J.G. Dunn, A.C. Chamberlain, J. Therm. Anal. 37 (1991) 1329–1346.
[5] J.G. Dunn, S.A.G. Jayaweera, S.G. Davies, Proc. Austral. Inst. Min. Met. 290(4) (1985) 75–82.
[6] G. Kullerud, R.A. Yund, J. Petrol. 3(1) (1962) l26–175.
[7] D.J. Vaughan, J.R. Craig, Mineral Chemistry of Metal Sulfides, Cambridge University Press, Melbourne, 1978.
[8] J.G. Dunn, S.G. Davies, Proc. Austral. Inst. Min. Met. 294 (1989) 57–62.
[9] J.G. Dunn, L.C. Mackey, J. Therm. Anal. 37 (1991) 2143–2164.
[10] J.G. Dunn, V.L. Howes, Thermochim. Acta 282/283 (1996) 305–316.
[11] P.G. Thornhill, L.M. Pidgeon, J. Metall. 9 (1957) 989–995.
[12] H. Tsukada, Z. Asaki, T. Tanabe, K. Kondo, Metall. Trans. B 12B (1981) 603–609.
[13] J.G. Dunn, Thermochim. Acta 300 (1997) 127–140.
[14] A.C. Chamberlain, J.G. Dunn, Thermochim. Acta 318 (1998) 101–113.
[15] J.G. Dunn, G.C. De, B.H. O'Connor, Thermochim. Acta 145 (1989) 115–130.
[16] J.G. Dunn, G.C. De, B.H. O'Connor, Thermochim. Acta 155 (1989) 135–149.
[17] F.R.A. Jorgensen, F.J. Moyle, J. Therm. Anal. 25 (1982) 473–485.
[18] F.R.A. Jorgensen, F.J. Moyle, J. Therm. Anal. 29 (1984) l3–17.